Structures, Energetics, and Transition States of the Silicon−Phosphorus Compounds Si_2PH_n (n = 7, 5, 3, 1). An ab Initio Molecular Orbital Study

Joanne M. Wittbrodt and H. Bernhard Schlegel*

Department of Chemistry, Wayne State University, Detroit, Michigan 48202

Received: June 7, 1999; In Final Form: August 17, 1999

This study examines a variety of compounds containing silicon−phosphorus multiple bonds as well as a selection of hydrogen-bridged species, including a doubly bridged structure. The structures of 29 minima and 37 transition states of the form Si_2PH_n (n = 7, 5, 3, 1) have been optimized at the MP2(full)/6-31G(d) level of theory; a representative subset was also optimized at the QCISD/6-311G(d,p) level. Relative energies were computed using a modification of the G2 level of theory. The stability of these compounds was investigated with respect to both unimolecular rearrangement and H_2 addition/elimination. Barrier heights for 1−2 and 1−3 H-shifts and for H_2 addition/elimination span wide ranges and are dependent on the nature of the bonding. Structures that contain true silicon−phosphorus double bonds are particularly stable with respect to unimolecular rearrangement.

Introduction

Interest in silicon−phosphorus chemistry has grown significantly in recent years. Nevertheless, much less is known experimentally about the structure and reactivity of Si−P bonds than other aspects of silicon chemistry.[1] A number of interesting Si−P analogues of hydrocarbon structures have been prepared, including cyclobutane,[2] bicyclobutane,[3] spiropentane,[4] hexane,[5] norbornane,[6] adamantane,[7] and cubane.[8] Compounds with Si═P double bonds are very reactive and can dimerize readily.[9,10] However, with bulky substituents, Si═P double bonded species can be stabilized sufficiently to permit spectroscopic characterization[11] and X-ray crystal structure analysis.[11−13] A computational study of the isomerization and unimolecular decomposition of Si−P−H systems would directly aid our understanding of Si−P compounds in inorganic chemistry.

Questions of silicon−phosphorus bonding also arise in the manufacture of electronic devices. Phosphorus-doped silicon is one of the principal n-type materials used for MOS gates in semiconductors. It can be formed by diffusion of dopants into the solid or by in situ doping using chemical vapor deposition (CVD) with a mixture of silane and phosphine.[14] However, some difficulties arise because phosphine tends to passivate the surface even at low concentrations,[15] resulting in a reduction of the deposition rate. This effect is much less severe when disilane is used as the silicon source. It has been suggested by Ahmed et al.[14] that this is due to the stronger adsorption of disilane to the surface. An alternative explanation is that silylene, produced along with silane in the decomposition of disilane, can adsorb to the surface with a sticking probability competitive with that of phosphine.[14,16] In the gas phase, silylene can easily insert into a phosphine PH bond, with a computed barrier height of less than 2 kcal/mol.[17,18] The product of this reaction, silylphosphine, has been observed experimentally in the pyrolysis of a phosphine/disilane mixture.[19] Thus the present theoretical study on Si−P bonding and reactivity could also contribute to our understanding of the gas-phase reactions in the CVD of phosphorus-doped silicon.

Early calculations by Gordon and co-workers[18] examined $SiPH_5$, $SiPH_3$, and SiPH as prototypes of single, double, and triple SiP bonds. Cowley and collaborators[20] studied various isomers of $SiPH_3$ to explore the stability of Si═P double bonds. Schleyer and Kost[21] calculated the bond energy of H_2Si═PH in a comparison of double-bond energies of second-row elements with carbon and silicon. Raghavachari et al.[17] investigated the insertion of silylene into various species, including PH_3. Mains et al.[22] examined the 1,1-elimination of H_2 from H_3SiPH_2 to form HSi═PH_2. A number of authors[23] have calculated ring strain energies of heterosubstituted cyclopolysilanes and have noted that cyclic SiH_2SiH_2PH and other monosubstituted three-membered polysilane rings have unusually short Si−Si bonds. Nyulászi et al.[24] have calculated $HSiPH_2$ and H_2SiPH in connection with a study of substituent effects on the stability of silylenes and silyl radicals. Schoeller and Busch[25] have computed the cations, radicals and anions of H_2SiP and $SiPH_2$. Hrušak et al.[26] have also examined cations and radicals in the H_2SiP system with ab initio and density functional methods. In the wake of recent experimental advances,[11−13] Driess and Janoschek[27] have also undertaken theoretical studies of H_2Si═PH and H_2Si═P−SiH_3.

There appear to be no systematic, experimental studies of the thermochemistry of silicon−phosphorus compounds. To fill this void, we recently calculated the structures, vibrational frequencies, and heats of formation for over 50 $Si_2P_mH_n$ molecules at the G2 level of theory.[28] This set is a comprehensive collection of all types of Si−P bonding and includes single and multiple bonds, radicals, triplets, silylenes, cyclic systems, and hydrogen-bridged species. A group additivity scheme has been developed that reproduces the heats of formation with a mean absolute deviation of 3.4 kcal/mol and can be used to describe bonding on surfaces and in solids, as well as in the gas phase. Zachariah and Melius[29] have also computed heats of formation for a number of Si−P−H species using the BAC-MP4 method (MP4/6-31G(d,p) with bond additivity corrections[30]). Their results compare well with our more accurate G2 calculations, with an average absolute difference of 2.7 kcal/

10.1021/jp9918510 CCC: $18.00
Published on Web 10/04/1999

mol. The largest error in the BAC-MP4 calculations is 8 kcal/mol for Si≡P. In the present work, we have used the G2 theory to calculate transition states for reactions connecting some of the more stable Si_2PH_n species.

Methods

Molecular orbital calculations were carried out with the Gaussian 98[31] series of programs using a variety of basis sets of split valence quality or better with multiple polarization and diffuse functions. Geometries were optimized by second-order Møller−Plesset perturbation theory (MP2(full)/6-31G(d)); a subset representing all of the major bonding motifs was also optimized at the QCISD(frozen core)/6-311G(d,p) level. A quasi-Newton optimization method was used to locate the minima, while the QST2 or QST3 methods[32] were used to locate many of the transition states. When the nature of the transition state was unclear, the reaction path following[33] was used to verify the connectivity. Some of the more difficult transition states were obtained using a combined method for the optimization of both transition states and points along the reaction path.[34] This method starts with an approximate *N*-point path which is iteratively relaxed until one of the points converges to a transition state, the end points converge to minima, and the remaining points converge to an approximate steepest descent path. In addition to locating transition states that resisted optimization by conventional methods, this approach occasionally identified unexpected intermediates along the path.

Vibrational frequencies and zero-point energies were calculated at the MP2(full)/6-31G(d) level using analytical second derivatives,[35] and thermal corrections to the energies were calculated by standard statistical thermodynamic methods.[36] Correlated energies were calculated by fourth-order Møller−Plesset perturbation theory[37] (MP4SDTQ, frozen core) and by quadratic configuration interaction with perturbative correction for triple excitations[38] (QCISD(T), frozen core) with the MP2-(full)/6-31G(d) optimized geometries. Relative energies were computed by the G2 method[39] (modified slightly, in that unscaled MP2 frequencies were used instead of Hartree−Fock, giving results within 0.8 kcal/mol of the regular G2 method). The energy computed at MP4/6-311G(d,p) was corrected for the effect of diffuse functions obtained at MP4/6-311+G(d,p), for the effect of higher polarization functions obtained at MP4/6-311G(2df,p), for the effect of electron correlation beyond fourth order obtained at QCISD(T)/6-311G(d,p), and for the inclusion of additional polarization functions at MP2/6-311+G-(3df,2p). Higher level corrections (HLC) for deficiencies in the wave function were estimated empirically[39] by comparing the calculated and experimental bond dissociation energies for 55 well-characterized molecules.

Results and Discussion

Figure 1 is a general map of the Si_2PH_n reactions considered in this work. Figure 2 shows some of the low-energy pathways from Si_2PH to Si_2PH_7. Structures are grouped according to the number of hydrogens and are labeled with the prefixes A, B, C, and D for $n = 7$, 5, 3, and 1, respectively. Within each of these sets, the labeling indicates the order of increasing energy. Energies are in kcal/mol relative to the lowest energy structure, $SiH_3-PH-SiH_3$, with H_2 molecules used to place the $n < 7$ structures on this scale. Transition states are labeled by the two structures that they connect. Unimolecular reactions are shown in Figures 3−8, with energies relative to the lowest energy isomer in each group. Hydrogen addition reactions appear in Figure 9. The Si−P bond lengths at the QCISD level of theory are on average 0.02 Å (0.8%) longer than the MP2 bond lengths with a standard deviation of 0.03 Å (1.2%), while the average difference in the Si−H and P−H bonds is ca. 0.01 Å (<1%). Since a variety of minima not included in the previous study have been found in this work, atomization energies, heats of formation, and entropies of all the Si_2PH_n ($n = 7$, 5, 3, 1) compounds are given in Table 1. Barriers for unimolecular reactions and H_2 additions are given in Tables 2 and 3, respectively. The differences between optimization at the MP2 and QCISD levels are examined in Table 4, where it is shown that the relative energies agree to within 0.5 kcal/mol, indicating that the MP2 structures are sufficiently accurate for the present work.

Si_2PH_7 (Figure 3). Simon et al.[19] have found evidence of these species in the mass spectral analysis of the pyrolysis of a phosphine/disilane mixture in an LPCVD reactor. Disilylphosphine (**A1**), which contains typical Si−P single bonds (ca. 2.25 Å), is the lowest energy isomer. The corresponding ylide (**A3**),

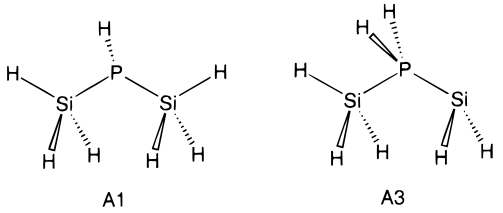

with one normal and one dative Si−P bond, is 35.8 kcal/mol higher in energy. This is in agreement with results from an earlier study[28] where SiH_2PH_3 was found to be 34.3 kcal/mol above silylphosphine. These isomers may be formed through the interaction of SiH_2 with silylphosphine, SiH_3PH_2, which itself is produced from the reaction of SiH_2 with phosphine and is observed in the copyrolysis of disilane and phosphine.[19] Here, the computed binding energy of SiH_2 and silylphosphine to form **A3** is 22.3 kcal/mol. This agrees well with binding energies reported for $SiH_2 + PH_3$: 21.2 kcal/mol in this work, 18−26 kcal/mol in the literature.[17,40]

Isomer **A1** can be reached from **A3** via a 1−2 H-shift, transition state (TS) **A3**−**A1**, with a 31.0 kcal/mol barrier. This is 9 kcal/mol lower than the analogous $SiPH_5$ barrier computed at a simpler level of theory (MP3/6-31G(d)//HF/3-21G) by Dykema et al.[18] However, since the binding energy of SiH_2 in **A3** is smaller than this barrier height, insertion of SiH_2 into a silylphosphine P−H bond may provide a lower energy pathway to **A1**. For the $SiPH_5$ system, the barrier for SiH_2 insertion into a phosphine P−H bond has been computed to be less than 2 kcal/mol.[17,18]

The $SiH_3SiH_2PH_2$ isomer (**A2**) is only 5.3 kcal/mol higher than **A1**, with no reasonable transition state to provide a connection (other than SiH_2 elimination and reinsertion). Isomer **A2** is easily reached from the higher energy **A4** via a 1−3

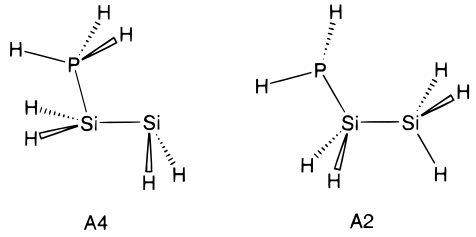

H-shift (TS **A4**−**A2**) with a barrier of 8.7 kcal/mol. Structure **A4** can be formed from SiH_2 and silylenephosphorane with a binding energy of 35 kcal/mol. As silylene accepts the silicon lone pair, the structure of the ylide moiety changes relatively

little. The H−Si−H angle widens by 8° and electron density in the Si−P bond shifts toward the silicon, increasing the bond length by 0.024 Å. Dissociation of **A4** into the products $PH_3 + Si_2H_4$ occurs with a small barrier, 4.5 kcal/mol, and is slightly exothermic, −1.3 kcal/mol.

Si_2PH_5. As shown in Figure 4, the lowest energy Si_2PH_5 isomer is a cyclic three-membered ring, **B1**. Only 2.3 kcal/mol above this is a phosphasilene, $H_3SiP{=}SiH_2$ (**B2**), with a silicon−

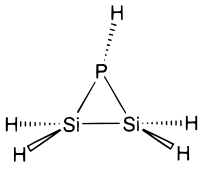

B1

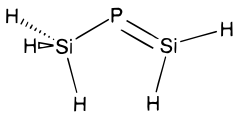

B2

phosphorus double bond. Driess et al. have synthesized compounds of the form **B2** with a variety substituents, including bulky sterically stabilizing groups, and have characterized them spectroscopically, chemically, and computationally.[13,27,41] Some of these compounds were found to be stable up to 90 °C.[41c] This is in good accord with one of the key findings of the present study, namely that the Si=P structure **B2** is calculated to be relatively stable with respect to unimolecular decomposition and rearrangement. Several pathways (Scheme 1) for the unimolecular reactions can be contemplated: simple bond cleavage, H_2 and SiH_2 eliminations, and 1−2 and 1−3 hydrogen shifts. Elimination of H_2 is endothermic by ca. 20 kcal/mol and has an overall barrier of 50 kcal/mol, as discussed below. Silylene elimination is endothermic by 60 kcal. The Si−P single- and double-bond cleavages are endothermic by 50 and 80 kcal/mol, respectively. Because these reactions are very endothermic, the related barriers were not examined as part of this study. This leaves hydrogen shift reactions as the most feasible routes for unimolecular reaction.

SCHEME 1

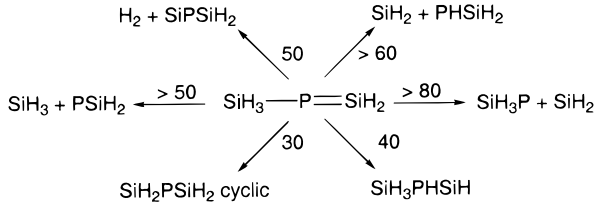

Conversion of **B2** to **B1** via a 1−2 H-shift across the Si−P single bond is impeded by a 33 kcal/mol barrier. In this ring-closing reaction (**B2**−**B1**), the Si−Si bond is almost fully formed in the TS, being only 0.03 Å longer than a typical acyclic Si−Si single bond. The shifting H atom is still significantly bonded to the silicon, but the Si−P bond is partially broken in the TS, with the distance 0.26 Å longer than a typical Si−P single bond. A 1−2 H-shift across the double bond (**B2**−**B6**) encounters an even larger barrier of 40 kcal/mol. The product of this reaction, **B6**, is discussed later in the text.

The smallest barrier from **B2** is 16 kcal/mol and leads to a symmetric H-bridged structure (**B5**) which lies only 4 kcal/mol below the **B2**−**B5** transition state. At the highest level of theory

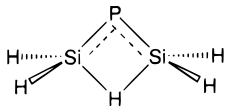

B5

used in the present work, this reaction is considerably more facile than predicted by Driess and Janoschek[27] (27 and 9 kcal/mol for the forward and reverse barriers, respectively, computed with pseudopotentials at the MP2 level of theory). Driess etal.[41a] also found a similar intermediate with fluorine in the bridging position in a theoretical examination of the 1−3 sigmatropic shift of fluorine in $FH_2SiP{=}SiH_2$.

Another phosphasilene, **B3**, with the silyl substituent on the silicon, lies less than 5 kcal/mol above **B2**. The Si=P bond is

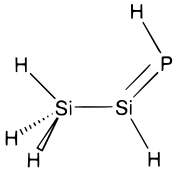

B3

ca. 0.02 Å longer than the double bond of **B2** but is still in the range of 2.062−2.094 Å found for Si=P in phosphasilene crystal structures.[11−13] The stability of **B3** is also comparable to that of **B2**, with a 39 kcal/mol barrier separating it from the lowest energy isomer. This transition state, **B3**−**B1**, involves a 1−2 hydrogen shift across the Si−Si single bond combined with ring closure. As the H atom transfers to the central silicon and breaks the Si−P double bond, it causes partial lone-pair density to appear on both the terminal Si and P. A bond then forms between these two atoms and the ring closes.

The lowest TS found from **B3**, 25 kcal/mol, connects to **B6** via a 1−2 silyl shift that is similar to the 1−2 H-shift separating **B6** and **B2** but has a relative energy that is 10 kcal/mol lower.

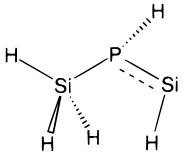

B6

This $SiH_3-PH{=}SiH$ structure is 14.2 kcal/mol above **B2** ($SiH_3-P{=}SiH_2$), in agreement with the previous study on both these and the related H_2P-SiH and $HP{=}SiH_2$ compounds, where the energy difference was found to be 13.8 and 14.3 kcal/mol, respectively.

Structure **B6** converts readily via **B4** to the lowest energy isomer, **B1**, with an overall barrier of only 2 kcal/mol. This provides alternate pathways from the phosphasilenes **B2** and **B3** to **B1**. In the case of **B2**, the overall barrier is 7 kcal/mol higher than the direct reaction. However, for **B3**, the pathway with **B6** as an intermediate has a barrier 13.5 kcal/mol lower than the direct reaction.

The 1−3 H shift in the reaction **B6**−**B1** is similar to the 1−3 sigmatropic H-shift, **B2**−**B2′**, in that an H-bridged intermediate is encountered (in the latter case **B5** and in the present case **B4**). This structure has two types of Si−P single bonds. One

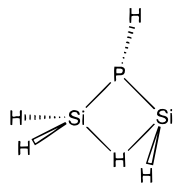

B4

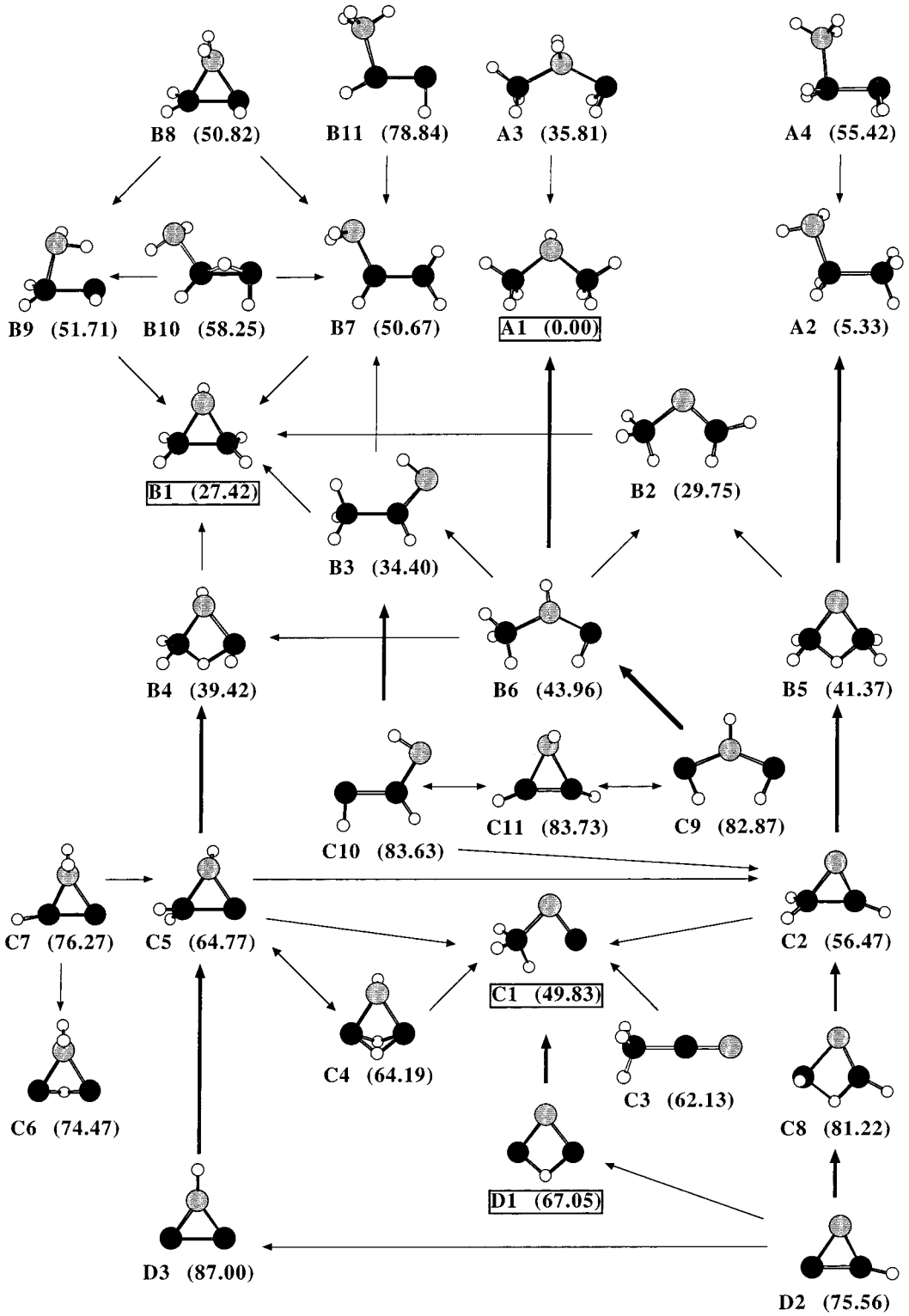

Figure 1. Equilibrium structures for Si_2PH_n optimized at the MP2(full)/6-31G(d) level of theory. Energies relative to **A1** were computed at the G2 level of theory with MP2(full)/6-31G(d) zero-point corrections.

bond is roughly 0.06 Å shorter than a normal Si−P single bond, indicative of some double-bond contribution from the phosphorus lone pair. The other bond is about 0.02 Å shorter than the 2.35 Å dative bonds found in **A3** and **A4**. This suggests that the structure could be a complex of $H_2Si{=}PH$ and SiH_2; however the binding energy is too high (50 kcal/mol) and there is substantial lone-pair density on the phosphorus.

The H-bridge in **B4** can be broken in two distinct places. Breaking the short Si−H bond gives rise to a 6.5 kcal/mol barrier leading to the lowest energy isomer, **B1**. As the H atom moves from the bridging position, both of the Si−P bonds become ca. 0.02 Å shorter. The shortening of the partial double bond in the TS occurs because the Si−Si bonding is not yet significant even though the Si−H bridge is already broken. Breaking the longer Si−H bond in **B4** leads to some difficulties. The MP2 level of theory predicts **B6** to be 1.1 kcal/mol lower in energy than **B4** with a 3.5 kcal/mol barrier. However, optimization at the QCISD/6-311G(d,p) level places **B6** 1.3 kcal/mol above **B4** with a smaller 1.7 kcal/mol barrier, while the more highly correlated G2 method places both **B4** and the TS

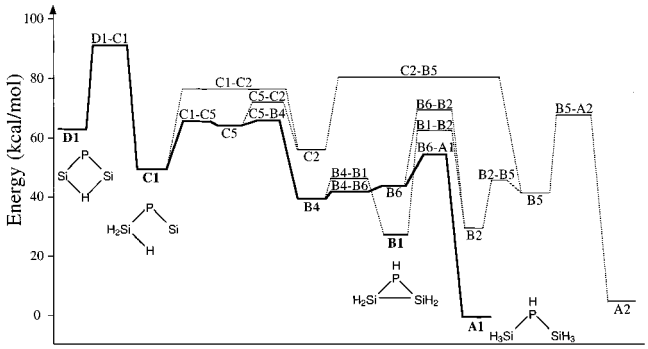

Figure 2. Relative energies for minima and transition states along some of the lower energy pathways connecting Si_2PH to Si_2PH_7. The bold line indicates the minimum-energy pathway. Energies were computed at the G2 level of theory with MP2(full)/6-31G(d) zero-point corrections.

below **B6** by 4.5 and 1.6 kcal/mol, respectively. This suggests that **B6** collapses directly to the H-bridged structure **B4**, from which there is only a 6.5 kcal/mol barrier to convert to **B1**.

The minima discussed so far have either no or one P−H bond. Four minima (**B7**−**B10**) with two P−H bonds were found 20−30 kcal/mol above the lowest energy isomer, **B1**. A $-PH_3$ structure, **B11**, lies an additional 20 kcal/mol above these $-PH_2$ structures (Figure 5). In **B11**, the Si−P dative bond is actually similar in length to a normal single bond, due to the electron-accepting ability of the terminal silicon atom. Extra lone-pair density on this atom is indicated by the 90° H−Si−Si angle. A 1−3 H-shift from phosphorus to the terminal silicon converts **B11** to **B7**, a PH_2-substituted silene, with a 16 kcal/mol barrier. The silene is particularly stable with respect to H-shift reactions from the $-PH_2$ group. The 1−3 H-shift, **B7′**−**B3**, has a barrier of 31 kcal/mol, while the 1−2 shift, **B7′**−**B1**, has a slightly larger barrier of 34 kcal/mol.

A substantially lower barrier, 12 kcal/mol, was found for **B7′**−**B10**, the key step in the overall 1−2 H-shift reaction, **B7′**−**B9**. In the intermediate, **B10**, the transferring H atom bridges the Si−Si bond which still retains partial double-bond character. The barrier to complete the reaction, **B10**−**B9**, is less than 2 kcal/mol. A higher energy pathway between **B7** and **B9** was found for the 1−2 shift of the PH_2 group. This reaction has an overall barrier of 17 kcal/mol and encounters the cyclic structure **B8** as an intermediate along the path. In either case, once **B9** is formed, there is only a 0.5 kcal/mol barrier (TS **B9**−**B1**) to transfer a hydrogen from the phosphorus to the terminal silicon and close the ring, suggesting that **B9** may not exist at higher levels of theory. A small or vanishing barrier is, however, consistent with the 2 kcal/mol barrier computed for the insertion of silylene into a phosphine P−H bond,[17,18] indicating that **B9**−**B1** can be viewed as a silylene insertion reaction.

Si_2PH_3. The three lowest isomers are good examples of Si−P multiple bonding (Figure 6). The most stable structure, H_3SiPSi (**C1**), contains a 2.069 Å Si−P double bond that is 0.012 Å

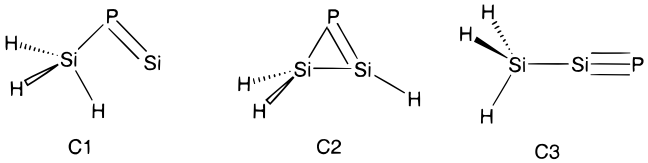

longer than the corresponding bond in the analogous HPSi structure.[28] Isomer **C2** is 7 kcal/mol higher and has a slightly longer Si−P double bond. The Si−P single bond is longer as well and there is substantial Si−Si double-bond character. This structure is well separated from **C1** by a 20 kcal/mol barrier for the 1−2 H-shift across the Si−Si bond. In this reaction, lone-pair density appears on the doubly bonded silicon as the transferring hydrogen bends toward the opposite silicon. This reduces the Si−Si bond to a single bond and temporarily shifts some of the Si−P double-bond character to the other Si−P bond.

Isomer **C3**, $H_3Si-Si{\equiv}P$, has a Si−P triple bond that is 0.013 Å longer than the corresponding bond in HSi≡P. There is an 8 kcal/mol barrier for a 1−2 silyl shift to form **C1**. In the **C3**−**C1** transition state, the linear Si−Si−P angle bends to 95°, the Si−Si bond lengthens by 0.04 Å, and the Si−P triple bond shortens by 0.01 Å before it undergoes the overall 0.072 Å increase to a double bond. Although the Si−P multiple bonds in this system are longer than those in the HSiP system, differences between the double- and triple-bond lengths are essentially the same, resulting in similar energetics. Isomers **C3** and **C1** are 12 kcal/mol apart, comparable to the 10 kcal/mol difference found in the HSiP system.[28]

The next lowest structures, isomers **C4** and **C5**, lie 14−15 kcal/mol above **C1**. The three-membered ring, **C5**, readily undergoes a 1−2 H-shift from the phosphorus to the SiH_2 group

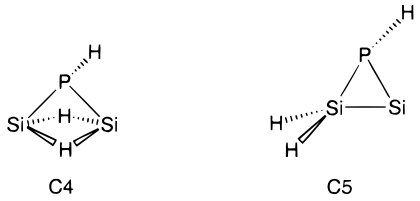

to form **C1** with only a 1 kcal/mol barrier. This reaction is facilitated by the shortening of the opposite Si−P bond in the TS as it converts to a double bond in the product. A larger barrier of 8 kcal/mol was found for the 1−2 shift in the opposite direction to form **C2**. Although a Si−P double bond is formed in this reaction as well, the barrier is larger because the H-shift occurs across this bond, lengthening it in the TS. In reverse, this reaction provides a pathway, **C2**−**C5**−**C1**, that has an overall barrier 4 kcal/mol lower that the 20 kcal/mol barrier for the direct **C2**−**C1** reaction. The doubly H-bridged form, **C4**, is reasonably stable, being separated from **C1** and **C5** by barriers of 24 and 11 kcal/mol, respectively. In the **C4**−**C5** transition state, both bridging H atoms transfer simultaneously to one of the silicon atoms. A similar barrier of 10 kcal/mol is found for the conversion of the singly H-bridged **C6** to the 2 kcal/mol higher three-membered ring, **C7**.

In the **C6**−**C7** TS, the Si−Si bond forms as one H−Si bond breaks and the corresponding Si−P bond lengthens. This

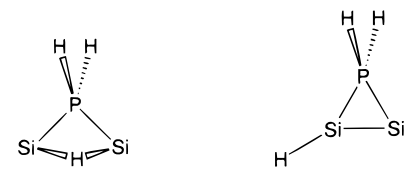

becomes a dative bond, while both Si−Si and HSi−P take on partial double-bond character in the product, **C7**. This isomer is also relatively stable, with a 12 kcal/mol barrier for the reaction **C7**−**C5**, a 1−2 H-shift from the phosphorus across the short Si−P bond. This bond is broken in the TS as the PH_2 group tips toward SiH. Meanwhile, the dative Si−P bond lengthens by 0.06 Å and the Si−Si double-bond character increases. Once the hydrogen is transferred, both Si−P distances

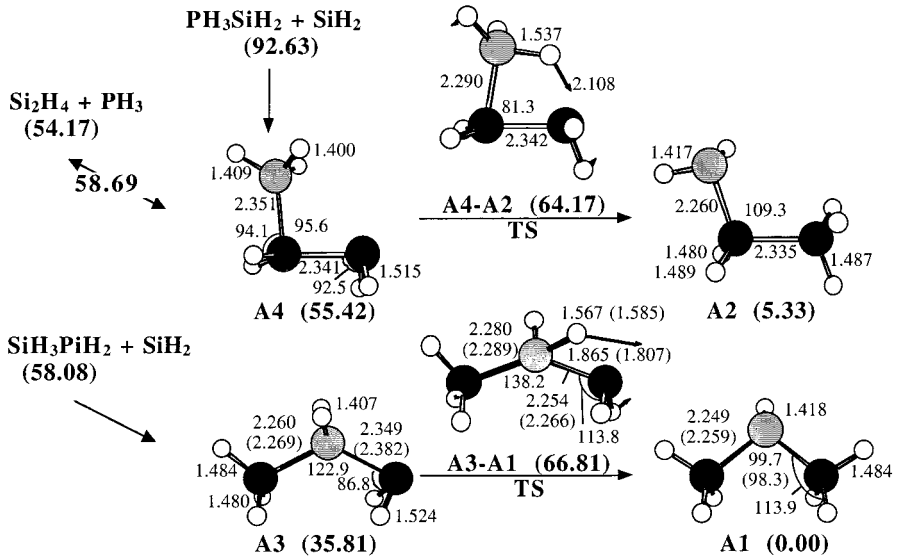

Figure 3. Si_2PH_5 isomers. Minima and transition states were optimized at the MP2(full)/6-31G(d) level of theory. (Numbers in parentheses refer to optimization at the QCISD(FC)/6-311G(d,p) level of theory.) Energies relative to **A1** were computed at the G2 level of theory with MP2(full)/6-31G(d) zero-point corrections.

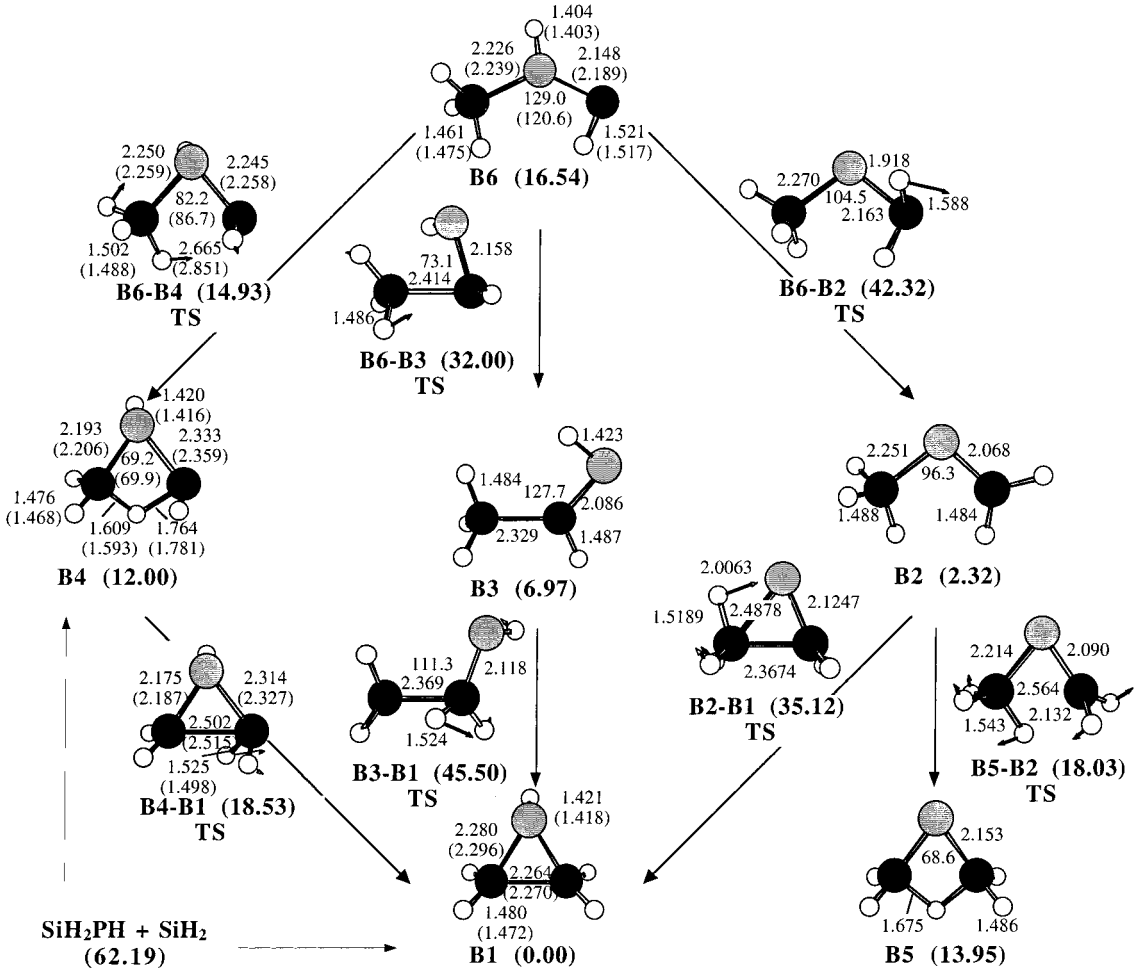

Figure 4. Low-energy Si_2PH_5 isomers. Minima and transition states were optimized at the MP2(full)/6-31G(d) level of theory. (Numbers in parentheses refer to optimization at the QCISD(FC)/6-311G(d,p) level of theory.) Energies relative to **B1** were computed at the G2 level of theory with MP2-(full)/6-31G(d) zero-point corrections.

shorten to partial double bonds and Si−Si lengthens to a single bond. As discussed above, transfer of the second hydrogen in PH_2, **C5**−**C1**, is much more facile.

Three closely related structures were found 33−34 kcal/mol above **C1** (Figure 7). In these isomers, **C9** through **C11**, each heavy atom is bonded to one hydrogen. The symmetric anti,-anti structure, **C9**, has a 5 kcal/mol barrier separating it from **C11**. The anti,syn isomer of **C9**, which is 0.8 kcal/mol higher in energy,[28] is an intermediate on the path. At the G2 level of theory, the **C11**−**C10** barrier disappears. (The MP2(full)/6-31G-

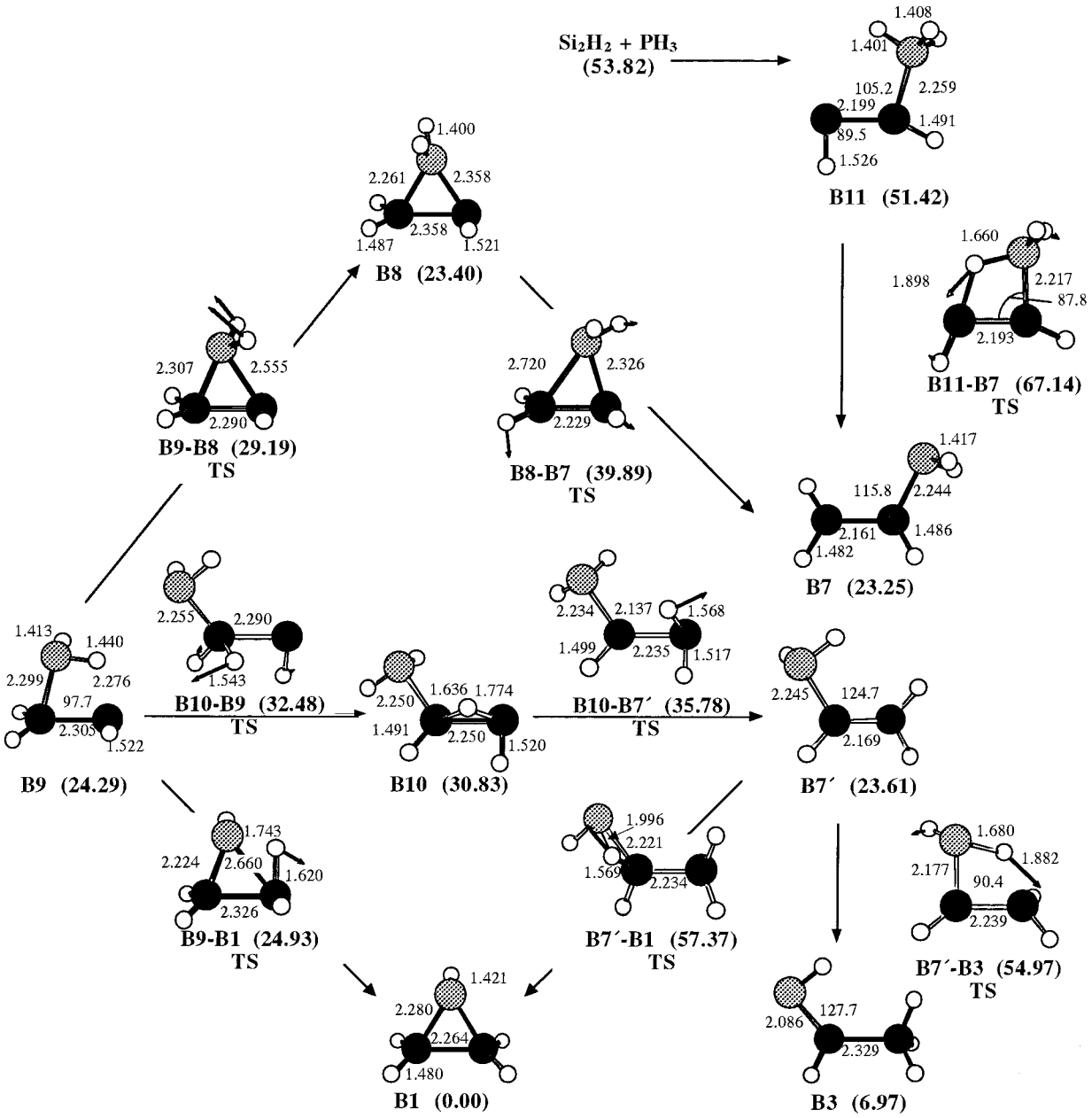

Figure 5. Higher energy Si_2PH_5 isomers. Minima and transition states were optimized at the MP2(full)/6-31G(d) level of theory. Energies relative to **B1** were computed at the G2 level of theory with MP2(full)/6-31G(d) zero-point corrections.

(d) barrier is 2 kcal/mol, while at QCISD/6-31G(d) it is only 0.5 kcal/mol.) These structures can readily convert to the second lowest energy isomer, **C2**, through the reaction **C10**−**C2**, a 1−3 H-shift accompanied by ring closure, with a 5 kcal/mol barrier.

Si_2PH (Figure 8). The lowest energy isomer, **D1**, is a four-membered ring with the H atom bridging the two Si atoms. The related nonbridged **D2** is 8.5 kcal/mol higher in energy.

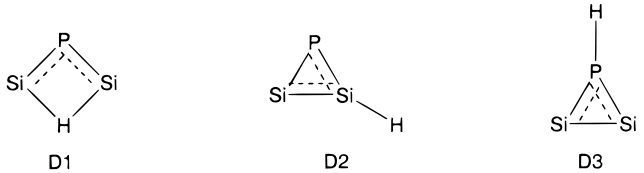

This structure is reasonably stable with a 18 kcal/mol barrier for insertion of the H atom into the Si−Si bond. Isomer **D3**, with two partial Si−P double bonds and an unusually long Si−Si single bond, is 11.5 kcal/mol above **D2** and is separated from it by an 8 kcal/mol barrier.

Unimolecular Reactions. The assorted unimolecular reactions discussed above are classified in Table 2, written in the exothermic direction. The 1−2 hydrogen shifts can be separated into two categories according to both barrier height and reactant type. The highest barriers, 24−38 kcal/mol, were found for cases in which the reactants were either acyclic or hydrogen-bridged structures. For some reactions, such as **B6**−**B2** and the H-bridged **C4**−**C1**, the barrier is lower than expected for a 1−2 H-shift because of exothermicity, which contributes to decreasing the barrier height. Lower barriers of 1−20 kcal/mol were found for reactants with cyclic Si−P−Si frameworks. These reactions may also be described as 1−3 H-shifts, which typically have lower barriers than 1−2 H-shifts. The highest barrier, 20 kcal/mol, was found for **C2**−**C1**, the only case in which a cyclic

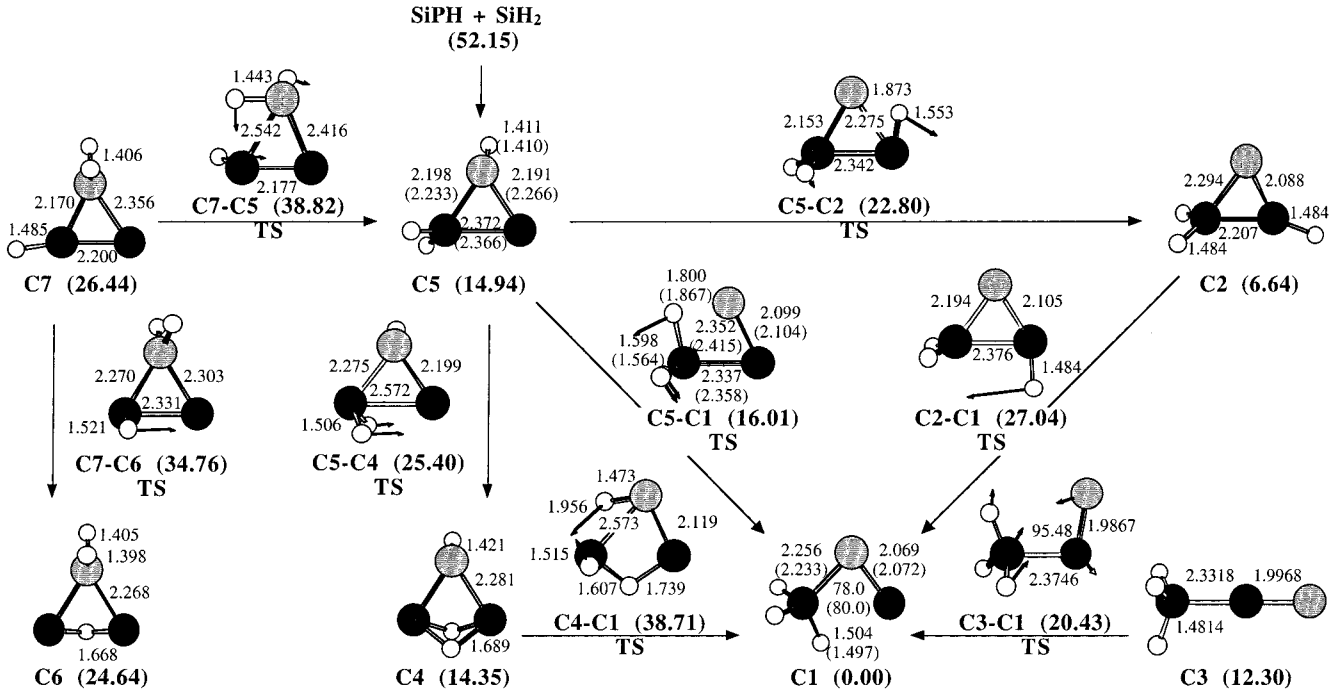

Figure 6. Low-energy Si_2PH_3 isomers. Minima and transition states were optimized at the MP2(full)/6-31G(d) level of theory. (Numbers in parentheses refer to optimization at the QCISD(FC)/6-311G(d,p) level of theory.) Energies relative to **C1** were computed at the G2 level of theory with MP2-(full)/6-31G(d) zero-point corrections.

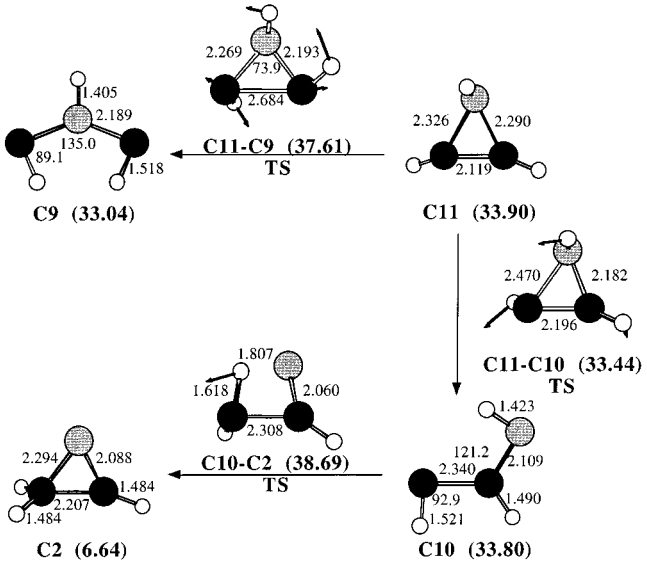

Figure 7. Higher energy Si_2PH_3 isomers. Minima and transition states were optimized at the MP2(full)/6-31G(d) level of theory. Energies relative to **C1** were computed at the G2 level of theory with MP2-(full)/6-31G(d) zero-point corrections.

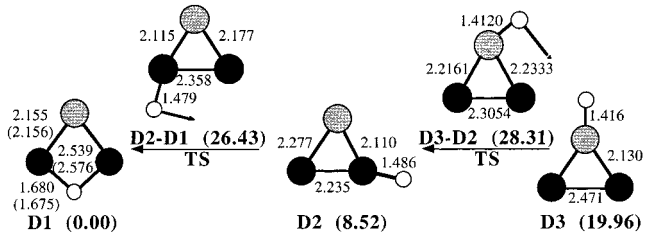

Figure 8. Si_2PH isomers. Minima and transition states were optimized at the MP2(full)/6-31G(d) level of theory. (Numbers in parentheses refer to optimization at the QCISD(FC)/6-311G(d,p) level of theory.) Energies relative to **D1** were computed at the G2 level of theory with MP2(full)/6-31G(d) zero-point corrections.

reactant possesses a full Si−P double bond, giving it extra stability. The lowest barrier, 1 kcal/mol, occurred for **C5**−**C1**, the most exothermic of the cyclic 1−2 H-shifts.

Barriers for hydrogen bridge formation by insertion into a Si−Si bond, 8−18 kcal/mol, fall into the same range as the 1−2 H-shifts with cyclic reactants. This is not surprising, since these reactions are essentially 1−2 shifts with the H-bridged structures formed as lower energy intermediates between cyclic reactants and their mirror image isomers. Reactions that break an H-bridge to form a lower energy product occur more easily, with barriers of 1.7−6.5 kcal/mol.

The 1−3 H-shifts listed in Table 2 all involve transfer of the hydrogen from the phosphorus on an acyclic P−Si−Si framework to the terminal silicon. The barrier height is strongly dependent on the nature of the Si−Si bond. The largest barrier, 31 kcal/mol, is found for **B7′**−**B3**, in which the Si−Si bond increases from 2.169 to 2.329 Å, whereas, the smallest barrier occurs in **C10**−**C2**, where the Si−Si bond decreases from 2.340 to 2.207 Å. Although the reaction **B9**−**B1** may be described as a 1−3 H-shift, both the low barrier and the structure of the reactant suggest that this is an example of a unimolecular silylene insertion.

H_2 Addition Reactions. The Si_2PH_n isomers with differing numbers of hydrogens are connected by H_2 addition reactions as shown in Figure 9 and Table 3. The simplest model for H_2 addition is $SiH_2 + H_2 \rightarrow SiH_4$. Jasinkski and Chu[42] performed an RRKM analysis of their pressure-dependent study of the $SiH_2 + H_2$ reaction and found the results at 300 K to be consistent with the 1.7 kcal/mol barrier computed by Gordon et al.[43] at the MP4/6-311++G(3df,3pd)// MP2/6-311G(2d,2p) level of theory. More detailed RRKM analyses[44] of the data indicated a lower activation energy of 0.3 kcal/mol. Using various density functional methods, Sosa and Lee[45] predict the $SiH_2 + H_2$ barrier to be -3.52 ± 3 kcal/mol. Calculations at the QCISD(T)/6-311++G(3df,2p)//MP2/6-31G(d,p) level of theory give a barrier of 4.2 kcal/mol, while the G2 method, which is an

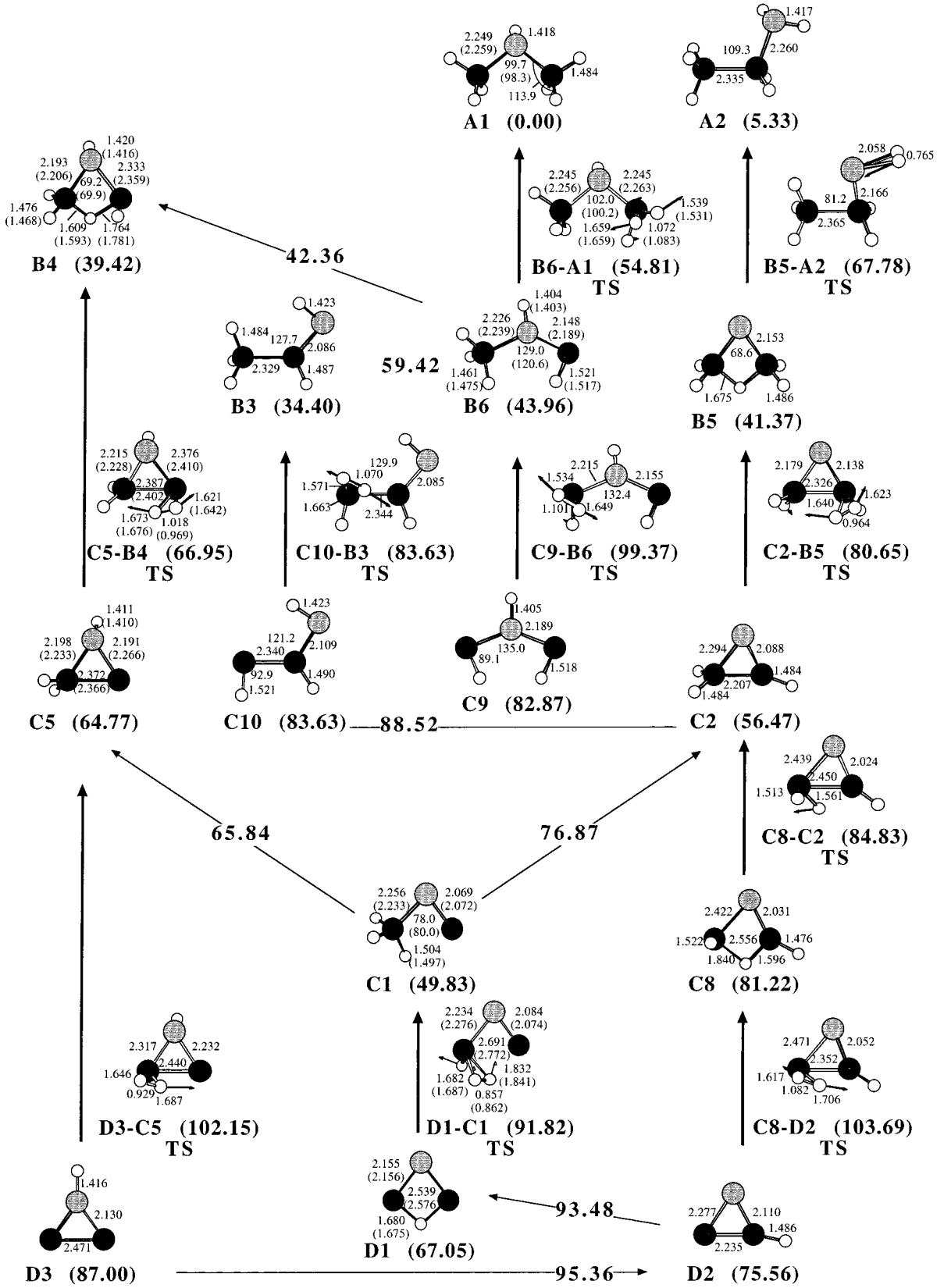

Figure 9. H_2 addition to Si_2PH_n. Minima and transition states for isomers were optimized at the MP2(full)/6-31G(d) level of theory. (Numbers in parentheses refer to optimization at the QCISD(FC)/6-311G(d,p) level of theory.) Energies relative to **A1** were computed at the G2 level of theory with MP2(full)/6-31G(d) zero-point corrections.

approximation of this level of theory, gives a value of 3.9 kcal/mol.[46] At the estimated QCISD(T)/6-311++G(3df,3pd) level of theory, the barrier is 2.9 kcal/mol.[46] Thus, on the basis of $SiH_2 + H_2$, one would expect very facile 1,1-addition of H_2 to unsaturated silicon in Si_2PH_n. However, as discussed below, this is not necessarily the case when there is significant interaction with neighboring groups.

The transition state with the lowest overall energy found connecting Si_2PH to Si_2PH_3 lies between the lowest energy forms, **D1** and **C1**, with a 24 kcal/mol barrier. This TS occurs

TABLE 1: Atomization Energies, Heats of Formation, and Entropies at the G2 Level of Theory

	structure[a]	atomization energy[c] (0 K)	heat of formation[d,e] 0 K	heat of formation[d,e] 298 K	entropy[e,f] (298 K)
A1	$SiH_3-PH-SiH_3$	632.8	20.2	15.7	81.3
A2	$SiH_3-SiH_2-PH_2$	627.6	25.5	21.0	81.2
A3	$SiH_3-PH_2-SiH_2$	597.2	55.9	51.5	81.8
A4	$SiH_2-SiH_2-PH_3$	577.7	75.3	71.1	84.6
B1	$SiH_2-PH-SiH_2$, **c**	501.8	48.0	44.6	72.4
B2	$SiH_3-P-SiH_2$	499.7	50.0	46.9	75.7
B3	$SiH_3-SiH-PH$	495.3	54.5	51.6	77.9
B4	$H-SiH_2-PH-SiH$, **hb**	489.6	60.1	56.6	71.9
B5	$H-SiH_2-P-SiH_2$, **hb**	487.6	62.2	58.5	70.0
B6	$SiH_3-PH-SiH$	485.8	63.9	61.1	80.2
B7	$SiH_2-SiH-PH_2$	479.2	70.6	67.8	78.2
B8	$SiH_2-SiH-PH_2$, **c**	478.6	71.2	68.0	73.8
B9	$SiH-SiH_2-PH_2$	477.9	71.9	68.9	76.3
B10[b]	$SiH-H-SiH-PH_2$, **hb**	471.3	78.4	75.4	77.1
B11	$SiH-SiH-PH_3$	451.0	98.8	96.0	79.1
C1	SiH_3-P-Si	376.4	70.1	68.5	71.9
C2	$SiH_2-P-SiH$, **c**	369.6	76.9	75.1	70.0
C3	SiH_3-Si-P	364.5	82.0	80.8	74.5
C4	$H_2-Si-PH-Si$, **2hb**	361.6	84.9	82.8	69.0
C5	$H_2Si-PH-Si$, **c**	361.5	85.0	83.4	71.5
C6	$H-Si-PH_2-Si$, **hb**	351.5	95.0	93.1	69.9
C7	$SiH-PH_2-Si$, **c**	349.9	96.6	94.9	71.2
C8	$H-SiH-P-SiH$, **hb**	345.2	101.3	99.9	72.7
C9	$SiH-PH-SiH$	343.7	102.8	101.5	73.9
C10	$SiH-SiH-PH$	343.0	103.5	102.3	75.6
C11	$SiH-PH-SiH$, **c**	342.7	103.8	102.4	72.4
D1	$H-Si-P-Si$, **hb**	255.7	87.5	87.2	67.1
D2	$SiH-P-Si$, **c**	247.4	95.8	95.7	68.2
D3	$Si-PH-Si$, **c**	236.0	107.2	107.1	68.6

[a] Cyclic and hydrogen-bridged structures are designated by **c** and **hb**, respectively. H-bridged species are four-membered rings unless otherwise noted. [b] The H-bridge is across the Si−Si bond, making a three-membered ring. [c] In kcal/mol with MP2(full)/6-31G(d) zero-point energies scaled by 0.9646.[48] [d] Heats of formation at 0 and 298 K are referenced to the following values in kcal/mol: 51.63 and 52.10 for H,[49] 75.42 and 75.62 for P,[49] 108.1 and 109.1 for Si.[50] [e] Thermal corrections were computed using unscaled MP2(full)/6-31G(d) frequencies. [f] In cal/(deg mol).

relatively early in the reaction, with the H−H bond 0.25 Å shorter and Si−H bonds 0.15−0.17 Å longer than the corresponding bonds in the $SiH_2 + H_2$ transition state. The TS for H_2 addition to **D2** is 12 kcal/mol higher in energy. This reaction, with a 28 kcal/mol barrier, connects **D2** to **C2** with **C8** as an intermediate. The **D2**−**C8** TS occurs later in the reaction than for **D1**−**C1**, with shorter Si−H and longer H−H distances. The H-bridged intermediate **C8**, formed by insertion of one of the adding H atoms into the Si−Si bond, is 22.5 kcal/mol below this TS. However, the barrier to break the H-bridge and reclose the ring is less than 4 kcal/mol. The **D2**−**C8**−**C2** connectivity was verified by the reaction path optimization technique[34] which encountered **C8** as an intermediate minimum in the attempt to find a TS between **D2** and **C2**. Addition of H_2 to isomer **D3** has the smallest barrier height, 15 kcal/mol. However, the overall energy of the TS, **D3**−**C5**, is only 1 kcal/mol lower than that of **D2**−**C8**. The barriers for H_2 addition to the Si_2PH isomers are much larger than the experimental 0.3−1.7 kcal/mol barrier for SiH_2 insertion into H_2[44] because the "empty" silicon p orbital actually contains significant electron density as evidenced by the partial Si−P double bonds in **D1**−**D3**. The barrier for H_2 1,1 -addition to **D2** is, however, ca. 10 kcal/mol smaller than the barrier for 1,2-addition of H_2 across a similar Si−Si double bond in disilene (39.5 kcal/mol, MP4/6-31G(d,p)//MP2/6-31G(d,p)).[47]

The main connection between Si_2PH_3 and Si_2PH_5 appears to be between **C5** and **B4**, with a 2 kcal/mol H_2 addition barrier.

TABLE 2: Barriers for Selected Unimolecular Rearrangements[a]

	barrier	figure		barrier	figure
1−2 H-Shift, Acyclic and H-Bridged reactants					
B3−**B1**	38.5	4	**A3**−**A1**	31.0	3
B7′−**B1**	33.8	5	**B6**−**B2**	25.8	4
B2−**B1**	32.8	4	**C4**−**C1**	24.4	6
1−2 H-Shift, Cyclic Reactants					
C2−**C1**	20.4	6	**C5**−**C2**	7.9	6
C7−**C5**	12.4	6	**C5**−**C1**	1.1	6
D3−**D2**	8.4	8			
1−2 H-Shift, Cyclic → H-Bridged Reactants					
D2−**D1**	17.9	8			
C5−**C4**[b]	10.5	6			
C7−**C6**	8.3	6			
1−3 H-Shift					
B7′−**B3**	31.4	5	**A4**−**A2**	8.7	3
B11−**B7**	15.7	5	**C10**−**C2**	4.9	7
1−2 Silyl Shift					
B6−**B3**	15.5	4	**C3**−**C1**	8.1	6
H−Bridge Breaking					
B4−**B1**	6.5	4	**C8**−**C2**[c]	3.6	9
B10−**B7′**	5.0	5	**B10**−**B9**	1.7	5
B5−**B2**	4.1	4			
Silylene Insertion					
B9−**B1**	0.6	5			

[a] Barrier heights are in kcal/mol. Reactions are presented in the exothermic direction. [b] Doubly bridged. [c] C8 is an H-bridged intermediate in the addition of H_2 to D2.

TABLE 3: Barriers for H_2 Addition[a]

reaction	barrier	reaction	barrier
C10−**B3**	0.0	**C2**−**B5**	24.2
C5−**B4**	2.2	**D1**−**C1**	24.8
		B5−**A2**[b]	26.4
B6−**A1**	10.8	**D2**−**C8**	28.1
D3−**C5**	15.2		
C9−**B6**	16.5		

[a] Barrier heights are in kcal/mol. Unless otherwise noted addition occurs at a silicon atom. [b] Addition at phosphorus.

TABLE 4: Comparison of QCISD/6-311G(d,p) Energies Using the MP2/6-31G(d) and QCISD/6-311G(d,p) Optimized Geometries

	relative energy[a]			relative energy[a]	
structure	MP2 opt	QCISD opt	structure	MP2 opt	QCISD opt
A1	0.00	0.00	**A3**−**A1**	73.19	73.53
A3	35.66	35.66	**B6**−**B4**	50.71	50.70
B1	35.62	35.58	**B4**−**B1**	58.01	58.51
B4	47.89	47.70	**C5**−**C1**	82.44	82.19
B6	49.17	48.98			
C1	62.81	62.55	**B6**−**A1**	61.31	61.30
C5	79.67	79.19	**C5**−**B4**	82.94	82.88
D1	87.56	87.45	**D1**−**C1**	113.05	112.71

[a] Energies are in kcal/mol relative to **A1**.

This reaction forms a hydrogen-bridged product, similar to **D2**−**C8** discussed above. However, the **C5**−**B4** barrier is much smaller because the insertion is now into a true Si−Si single bond (2.37 Å) as opposed to the partial double bond (2.24 Å) of **D2**. Furthermore, the overall energy required for **C5**−**B4** is 17 kcal/mol less than needed for **C10**−**B3**, for which there is essentially no barrier. These 0−2 kcal/mol barriers for H_2 addition to **C10** and **C5** compare well with experimental and theoretical barriers for the $SiH_2 + H_2$ insertion reaction.[42−46] This behavior is easily understood for **C10** from its silylene-like structure, with an Si−Si single bond. However, the cause

for the low addition barrier to **C5** is not as readily apparent. The partial Si−P bond on the reactive silicon in **C5** suggests that the barrier should be similar to the 15−18 kcal/mol barriers found for H_2 addition to the Si_2PH isomers. However, in the **C5**−**B4** TS, the partial Si−P double bond becomes 0.12 Å longer than a typical Si−P single bond. This behavior gives rise to the small 2 kcal/mol barrier and is related to the formation of the H-bridge in the product, **B4**, which, as discussed above, can readily isomerize to **B1** with a barrier of 6.5 kcal/mol. In **C9**, the allylic nature of the π system, with partial Si−P double bonds, hinders H_2 addition, giving rise to a 16 kcal/mol barrier. An even larger barrier of 26 kcal/mol is found for H_2 addition to **C2**, where the silicon reaction site is not electron deficient. Here the Si−P double bond must be broken before H_2 can interact with the silicon p orbital.

Two H_2 addition reactions were found connecting Si_2PH_5 to Si_2PH_7. The smallest barrier, 11 kcal/mol, is for **B6**−**A1**, forming the lowest energy structure SiH_3PHSiH_3. This is 5.7 kcal/mol smaller than the barrier for the addition to the allylic **C9**. However, the barrier does not vanish since there is still substantial Si−P double-bond character on the reactive silicon. The reverse barrier of 55 kcal/mol for **B6**−**A1**, the 1,1-elimination of H_2 from SiH_3PHSiH_3, agrees well with the 58 kcal/mol barrier found by Mains et al.[22] for H_2 elimination from SiH_3PH_2. The second reaction, **B5**−**A2**, involves hydrogen addition to phosphorus combined with ring opening. In this TS, with a 26 kcal/mol barrier, the bridging H transfers to one of the silicon atoms and the corresponding Si−P bond breaks before any significant interaction occurs between the phosphorus atom and the adding hydrogens.

Conclusions

This study has examined the stability of 29 minima in the Si_2PH_n (n = 7, 5, 3, 1) system with respect to unimolecular rearrangement and H_2 addition. Compounds in this work include examples of silicon−phosphorus multiple bonds and hydrogen bridging. Structures **B2**, **B3**, **C1**, and **C2** contain silicon−phosphorus bonds that lie within the range of 2.062−2.094 Å found for Si−P double bonds in crystal structures[11−13] and are particularly stable with respect to unimolecular rearrangement. The phosphasilenes **B2** and **B3** have barriers in excess of 25 kcal/mol along both direct and indirect routes to **B1**, the lowest energy Si_2PH_5 structure. The cyclic structure **C2** is separated from **C1**, the lowest of the Si_2PH_3 isomers, by barriers of 16−20 kcal/mol. Structures containing partial Si−P double bonds are typically less stable, as exemplified by the comparison of the 1−3 H-shifts from the silyl groups in $SiH_3-PH{=}SiH$ (**B6**) and $SiH_3-P{=}SiH_2$ (**B2**). In each case, there is an H-bridged intermediate (**B4** and **B5**, respectively) from which the barrier to completion is 4−5 kcal/mol. However, the former case has only a partial Si−P double bond and **B6** is predicted to collapse with no barrier to the intermediate **B4**. In the latter, **B2** has a full double bond and **B2**−**B5** is endothermic with a 16 kcal/mol barrier.

Acknowledgment. This work was supported by a grant from the National Science Foundation (CHE 9400678).

Supporting Information Available: Listings of Cartesian coordinates and energies for the minima and transition states at the MP2(full)/6-31G(d) level of theory. This material is available free of charge via the Internet at http://pubs.acs.org.

References and Notes

(1) Armitage, D. A. In *The Silicon-Heteroatom Bond*; Patai, S., Rappoport, Z., Eds.; Wiley: New York, 1989, 1991.
(2) Clegg, W.; Haase, M.; Klingebiel, U. K.; Sherldrick, G. M. *Chem. Ber.* **1983**, *116*, 146.
(3) Driess, M.; Pritzkow, H.; Reisgys, M. *Chem. Ber.* **1991**, *124*, 1923.
(4) Tebbe, K.-F.; Heinlein, T. *Z. Anorg. Allg. Chem.* **1984**, *515*, 7.
(5) Driess, M.; Reisgys, M.; Pritzkow, H. *Angew. Chem., Int. Ed. Engl.* **1992**, *31*, 1510.
(6) Honle, W.; von Schnering, H. G. *Z. Anorg. Allg. Chem.* **1978**, *442*, 107.
(7) (a) Honle, W.; von Schnering, H. G. *Z. Anorg. Allg. Chem.* **1978**, *442*, 91. (b) Baudler, M.; Oehlert, W.; Tebbe, K.-F. *Z. Anorg. Allg. Chem.* **1991**, *598*, 9.
(8) Baudler, M.; Scholz, G.; Tebbe, K.-F.; Feher, M. *Angew. Chem., Int. Ed. Engl.* **1989**, *28*, 339.
(9) Couret, C.; Escudie, J.; Satge, J.; Andriamizaka, J. D.; Saint-Roche, B. *J. Organomet. Chem.* **1979**, *182*, 9.
(10) Lefèvre, V.; Ripoll, J. L.; Dat, Y.; Joantéguy, S.; Métail, V.; Chrostowska-Senio, A.; Pfister-Guillouzo, G. *Organometallics* **1997**, *16*, 1635.
(11) (a) Smit, C. N.; Lock, F. M.; Bickelhaupt, F. *Tetrahedron Lett.* **1984**, *25*, 3011. (b) Smit, C. N.; Bickelhaupt, F. *Organometallics* **1987**, *6*, 1156. (c) van den Winkel, Y.; Bastiaans, H. M. M.; Bickelhaupt, F. *J. Organomet. Chem.* **1991**, *405*, 183.
(12) Bender, H. R. G.; Niecke, E.; Nieger, M. *J. Am. Chem. Soc.* **1993**, *115*, 3314.
(13) Driess, M.; Rell, S.; Pritzkow, H. *J. Chem. Soc., Chem. Commun.* **1995**, 253.
(14) Ahmed, W.; Ahmed, E.; Hitchman, M. L. *J. Mater. Sci.* **1995**, *30*, 4115.
(15) (a) Hamers, R. J.; Wang, Y. *Chem. Rev.* **1996**, *96*, 1261. (b) Waltenburg, H. N.; Yates, J. T., Jr.; *Chem. Rev.* **1995**, *95*, 1589.
(16) Grahn, J. V.; Pejnefors, J.; Sandén, M.; Zhang, S.-L.; Östling, M. *J. Electrochem. Soc.* **1997**, *144*, 3952.
(17) Raghavachari, K.; Chandrasekhar, J.; Gordon, M. S.; Dykema, K. J. *J. Am. Chem. Soc.* **1984**, *106*, 5853.
(18) Dykema, K. J.; Truong, T. N.; Gordon, M. S. *J. Am. Chem. Soc.* **1985**, *107*, 4535.
(19) Simon, J.; Feurer, R.; Reynes, A.; Morancho, R. *J. Anal. Appl. Pyrolysis* **1993**, *26*, 27.
(20) Lee, J.-G.; Boggs, J. E.; Cowley, A. H. *J. Chem. Soc., Chem. Commun.* **1985**, 773.
(21) Schleyer, P. v. R.; Kost, D. *J. Am. Chem. Soc.* **1988**, *110*, 2105.
(22) Mains, G. J.; Trachtman, M.; Bock, C. W. *J. Mol. Struct.* **1991**, *231*, 125.
(23) (a) Grev, R. S.; Schaefer, H. F. *J. Am. Chem. Soc.* **1987**, *109*, 6577. (b) Cremer, D.; Gauss, J.; Cremer E. *J. Mol. Struct.* **1988**, *169*, 531. (c) Boatz, J. A.; Gordon, M. S. *J. Phys. Chem.* **1989**, *93*, 3025.
(24) Nyulászi, L.; Belghazi, A.; Szétsi, S. K.; Veszprémi, T.; Heinicke, J. *J. Mol. Struct.* **1994**, *313*, 73.
(25) Schoeller, W. W.; Busch, T. *J. Mol. Struct.* **1994**, *313*, 27.
(26) Hrušak, J.; Schroder, D.; Schwarz, H.; Iwata, S. *Bull. Chem. Soc. Jpn.* **1997**, *70*, 777.
(27) Driess, M.; Janoschek, R. *J. Mol. Struct.* **1994**, *313*, 129.
(28) Baboul, A. G.; Schlegel, H. B. *J. Am. Chem. Soc.* **1996**, *118*, 8444.
(29) Zachariah, M. R.; Melius, C. F. *J. Phys. Chem. A* **1997**, *101*, 913.
(30) Melius, C. F.; Binkley, J. S. *Symp. (Int.) Combust. [Proc.]* **1986**, *21*, 1953.
(31) Frisch, M. J.; Trucks, G. W.; Schlegel, H. B.; Scuseria, G. E.; Robb, M. A.; Cheeseman, J. R.; Zakrzewski, V. G.; Montgomery, J. A.; Stratmann, R. E.; Burant, J. C.; Dapprich, S.; Millam, J. M.; Daniels, A. D.; Kudin, K. N.; Strain, M. C.; Farkas, O.; Tomasi, J.; Barone, V.; Cossi, M.; Cammi, R.; Mennucci, B.; Pomelli, C.; Adamo, C.; Clifford, S.; Ochterski, J.; Petersson, G. A.; Ayala, P. Y.; Cui, Q.; Morokuma, K.; Malick, D. K.; Rabuck, A. D.; Raghavachari, K.; Foresman, J. B.; Cioslowski, J.; Ortiz, J. V.; Stefanov, B. B.; Liu, G.; Liashenko, A.; Piskorz, P.; Komaromi, I.; Gomperts, R.; Martin, R. L.; Fox, D. J.; Keith, T.; Al-Laham, M. A.; Peng, C. Y.; Nanayakkara, A.; Gonzalez, C.; Challacombe, M.; Gill, P. M. W.; Johnson, B. G.; Chen, W.; Wong, M. W.; Andres, J. L.; Head-Gordon, M.; Replogle, E. S.; Pople, J. A. *Gaussian 98*, Revision A.2; Gaussian, Inc.: Pittsburgh, PA, 1998.
(32) Peng, C.; Schlegel, H. B. *Isr. J. Chem.* **1994**, *33*, 449.
(33) (a) Gonzalez, C.; Schlegel, H. B. *J. Chem. Phys.* **1989**, *90*, 2154. (b) Gonzalez, C.; Schlegel, H. B. *J. Phys. Chem.* **1990**, *94*, 5523.
(34) Ayala, P. Y.; Schlegel, H. B. *J. Chem. Phys.* **1997**, *107*, 375.
(35) (a) Pople, J. A.; Krishnan, R.; Schlegel, H. B.; Binkley, J. S. *Int. J. Quantum Chem., Quantum Chem. Symp.* **1979**, *13*, 225. (b) Handy, N. C.; Amos, R. D.; Gaw, J. F.; Rice, J. E.; Simandiras, E. D. *Chem. Phys. Lett.* **1985**, *120*, 151. (c) Trucks, G. W.; Frisch, M. J.; Andres, J. L.; Schlegel, H. B. In preparation.
(36) McQuarrie, D. A. *Statistical Thermodynamics*; University Science Books: Mill Valley, CA, 1973.
(37) (a) Krishnan, R.; Pople, J. A. *Int. J. Quantum Chem.* **1978**, *14*, 91. (b) Cremer, D. Møller-Plesset Perturbation Theory. In *Encyclopedia of Computational Chemistry*; Schleyer, P. v. R., Allinger, N. L., Clark, T.,

Gasteiger, J., Kollman, P. A., Schaefer, H. F., III; Schreiner, P. R., Eds. Wiley: Chichester, U.K., 1998.

(38) Pople, J. A.; Head-Gordon, M.; Raghavachari, K. *J. Chem. Phys.* **1987**, *87*, 5968.

(39) (a) Curtiss, L. A.; Raghavachari, K.; Trucks, G. W.; Pople, J. A. *J. Chem. Phys.* **1991**, *94*, 7221. (b) Curtiss, L. A.; Carpenter, J. E.; Raghavachari, K.; Pople, J. A. *J. Chem. Phys.* **1992**, *96*, 9030. (c) Raghavachari, K.; Curtiss, L. A. In *Modern Electronic Structure Theory*; Yarkony, D. R., Ed.; World Scientific Publishing: Singapore, 1995; p 459.

(40) Schoeller, W. W.; Schneider, R. *Chem. Ber.* **1997**, *130*, 1013.

(41) (a) Driess, M.; Rell, S.; Pritzkow, H.; Janoschek, R. *Angew. Chem., Int. Ed. Engl.* **1997**, *36*, 1326. (b) Driess, M.; Pritzkow, H.; Rell, S. *Organometallics* **1996**, *15*, 1845. (c) Driess, M. *Angew. Chem., Int. Ed. Engl.* **1991**, *30*, 1022.

(42) Jasinski, J. M.; Chu, J. O. *J. Chem. Phys.* **1988**, *83*, 1678.

(43) Gordon, M. S.; Gano, D. R.; Binkley, J. S.; Frisch, M. J. *J. Am. Chem. Soc.* **1986**, *108*, 2191.

(44) (a) Moffat, H. K.; Jensen, K. F.; Carr, R. W. *J. Phys. Chem.* **1991**, *95*, 145. (b) Mick, H. J.; Roth, P.; Smirnov, V. N. *Kinet. Catal.* **1996**, *37*, 1.

(45) Sosa, C.; Lee, C. *J. Chem. Phys.* **1993**, *98*, 8004.

(46) Su, M.-D.; Schlegel, H. B. *J. Phys. Chem.* **1993**, *97*, 9981.

(47) Sakai, S. *J. Phys. Chem. A* **1997**, *101*, 1140.

(48) Pople, J. A.; Scott, A. P.; Wong, M. W.; Radom, L. *Isr. J. Chem.* **1993**, *33*, 345.

(49) Chase, M. W.; Davies, C. A.; Downey, J. R.; Frurip, D. J.; McDonald, R. A.; Szverud, A. N. *J. Phys. Chem. Ref. Data* **1985**, *14*.

(50) (a) Grev, R. S.; Schaefer, H. F. *J. Chem. Phys.* **1992**, *97*, 8389. (b) Ochterski, J. W.; Petersson, G. A.; Wiberg, K. B *J. Am. Chem. Soc.* **1995**, *117*, 11299.